Formation Mechanism and Anatomical Structure of the Knee Roots of Taxodium Ascendens

Zhuangzhuang Qian
Co-Innovation Center for Sustainable Forestry in Southern China, College of Forestry, Nanjing Forestry University, Nanjing 210037, PR China

Lin Wu
Co-Innovation Center for Sustainable Forestry in Southern China, College of Forestry, Nanjing Forestry University, Nanjing 210037, PR China

Luozhong Tang (luozhongtang@njfu.edu.cn)
Nanjing Forestry University

Research Article

Keywords: anatomic structure, ethylene, flooding, formation mechanism, knee root, Taxodium ascendens

Posted Date: May 27th, 2021

DOI: https://doi.org/10.21203/rs.3.rs-533919/v1

Formation mechanism and anatomical structure of the knee roots of *Taxodium ascendens*

Zhuangzhuang Qian; Lin Wu; Luozhong Tang*

Co-Innovation Center for Sustainable Forestry in Southern China, College of Forestry, Nanjing Forestry University, Nanjing 210037, PR China

Corresponding author:

Dr. Luozhong Tang

Co-Innovation Center for Sustainable Forestry in Southern China, College of Forestry, Nanjing Forestry University, Nanjing 210037, PR China

159 Longpan Road, Nanjing 210037, PR China

E-mail address: luozhongtang@njfu.edu.cn

Tel: 86-025-85427325

Fax: 86-025-85428883

Abstract

Aims: Flooding seriously limits the growth and distribution of plants. *Taxodium ascendens* is a typical tree species with high flood tolerance, and it can generate knee roots in the wetlands. This study was conducted to understand the formation mechanism of the knee roots.

Methods: The number and size of knee roots and soil flooding conditions were investigated in this study. Furthermore, physiology, biochemical responses, and the anatomical structure of knee roots and underground roots were measured at different developmental stages.

Results: The results show that the formation of knee roots was significantly affected by the soil water table ($P < 0.05$). Moreover, knee root formation was affected by ethylene and indole-3-acetic acid (IAA) concentrations in the roots. The 1-aminocyclopropane-1-carboxylic acid (ACC) content and ACC synthase activity were significantly lower in the knee roots than in the underground roots. The ethylene release rate was significantly higher in the knee roots than in the underground roots ($P < 0.05$), and IAA content first increased and then decreased with knee root development. The cells of the periderm at the apex of the knee roots were dead and had a large number of intercellular spaces, which was beneficial for the growth of *T. ascendens*.

Conclusions: Seasonal flooding induced the production of endogenous hormones, resulting in the formation of knee roots, which improved root respiration and ventilation. The results obtained can gain a basis for the formation mechanism of knee roots and provide scientific evidence for the afforestation and management under wetland conditions.

Keywords: anatomic structure; ethylene; flooding; formation mechanism; knee root; *Taxodium ascendens*

Introduction

Nowadays, flood damage is receiving a lot of attention, as flooding and waterlogging phenomena tend to be closely associated with global climate changes (Hirabayashi et al. 2013, Zhou et al. 2020). Flooding and submergence are major abiotic stresses that determine species distribution, growth, and yield (Sairam et al. 2008, Herzog et al. 2016). In China, about 6.6×10^5 km^2 land is waterlogged, accounting for 6.6% of the total land area; in 2020, 16 provinces and 11.22 million people were adversely affected by floods. Uneven precipitation and poor drainage result in frequent waterlogging, which can seriously constrain crop growth and productivity (Kuai et al. 2015, Liu et al. 2019, Xiong et al. 2019). Therefore, selection of a suitable farmland shelter forest is important. Flooding stress restricts the diffusion of oxygen in plant tissues, which seriously affects plant growth (Voesenek and Baileyserres 2013). Flood-tolerant plant species have a series of adaptive mechanisms, such as morphological changes and physiological and biochemical reactions, that can protect the plants from flooding stress (Khan et al. 2020). The responses of the roots to flood environments reflect the adaptability of a tree to waterlogging (Blom and Voesenek 1996). For example, the structures of some Chenopodiaceae roots change to the herring-bone shape to consume less oxygen and avoid being damaged by toxins (Bouma et al. 2001). The red mangrove (*Rhizophora mangle*) in coastal intertidal zones has a conspicuous system of stilt-like roots that grow from the main stem and resemble flying buttresses with developed leaf aerenchyma for gas exchange and prevention of oxygen loss during flooding stress (Lance and Alison 2010, Mendez-Alonzo et al. 2015). *Avicennia marina* can develop finger-like pneumatophores to obtain oxygen for its underground root system and sustain hypoxic

64 conditions (Purnobasuki et al. 2017). *Eucalyptus camaldulensis and Eucalyptus globulus* can produce
65 numerous white adventitious roots that float on the water surface to obtain more oxygen (Sena Gomes
66 and Kozlowski 1980).

67 *Taxodium ascendens* is a water-tolerant species that is widely distributed in the subtropical
68 riversides and drawdown areas of reservoirs and ponds in China (Yi et al. 2008, Li et al. 2010).
69 *Taxodium ascendens* develops knee roots to increase water tolerance under flooding conditions, and it
70 is widely cultivated in farmland shelter forests and as a roadside tree (Tang et al. 2008, Du et al. 2010).
71 Sakio and Yamamoto (2002) have reported that only some specific flood-tolerant plant species like *T.*
72 *ascendens*, *Taxodium distichum*, and *Glyptostrobus pensilis* develop knee roots.

73 Although various studies have reported the effects of waterlogging on the metabolic and
74 physiochemical characteristics of different trees, most of the studies were conducted in greenhouses
75 and focused on tree seedlings (Conner et al. 1997, Andrson and Pezeshki 1999, Li et al. 2010, Wang et
76 al. 2016) and few studies were performed using adult trees under field conditions. Therefore, the
77 formation mechanism of aerial and knee roots, which are generated in only adult trees, have not yet
78 been elucidated. Moreover, the adaptation mechanism of roots that respond to waterlogging stress is
79 unclear. Yamamoto (1992) reported that the depth of flooding affects the formation of knee roots and
80 hypothesized the interaction between ethylene and indole-3-acetic acid (IAA) in knee root production.
81 Ethylene plays an important role in promoting plant growth and seed germination and enhancing
82 anoxia resistance. Especially, ethylene, as an internal gaseous signal, is used by plants to sense shifts

from aerial to aquatic environments and induce changes in plant morphology and anatomy (Visser and Voesenek 2004, Jackson 2007). Sundberg et al. (1991) indicated that endogenous IAA is a key regulator of the development of the secondary vascular tube, and it has significant effects on cambial activity and development. 1-Aminocyclopropane-1-carboxylic acid (ACC) synthetase and ACC oxidase are essential enzymes that participate in the conversion of ACC to ethylene (Dong et al. 1992, Vall-llaura et al. 2020).

Therefore, we hypothesized that the formation of knee roots was associated with the flooding condition, and induced by endogenous hormones. In this study, the water table, ethylene and relative enzymes, IAA content, and anatomical structure of knee roots and conventional underground roots of *T. ascendens* were evaluated. The objective of this study was to compare the differences in endogenous hormones between the knee roots developed from underground roots and conventional underground roots, to understand the adaptation mechanism of *T. ascendens* under flooding conditions and form a basis for afforestation management under wetland conditions.

Materials and methods

Research site

The study was performed in a 28-year-old *Taxodium ascendens* forest plantation (approximately 500 hectares). The plantation was cultivated in a wetland at the Zhaoguan Forest Farm (N32°31′41″ and E119°30′35″), Jiangdu County, Jiangsu Province, China, and the plant spacing was 1.5 m × 4 m.

The average tree diameter at breast height (DBH) and tree height were 25.75 cm and 14.33 m, respectively. The soil type was paddy soil with poor air permeability.

Three experimental sites were chosen on the basis of the soil water table: high water table site (the flooding period was more than 3 months from June to September, maximum submergence depth was about 0.8 m, and annual average water table was more than -0.6 m), middle water table site (the flooding period was 1 to 2 months from July to August, maximum submergence depth was about 0.2 m, and annual average water table was from -0.6 m to -1.2 m), and low water table site (no flooding status, and the annual average water table was less than -1.2 m). A total of 21 plots (7 sampling plots at each water-table site) were established, and each plot was 96 m^2 (8 × 12 m).

Analysis of the soil water table and knee root number and size

The soil water table at each site was measured every mid-month from Oct 2011 to Oct 2016. The tree height, DBH, and number and size of knee roots were measured in October 2016.

Polyethylene pipes (length, 2 m; inner diameter, 11 cm) were used to investigate the soil water table. The pipes were drilled with 4 mm diameter holes (the spacing between each hole was 5 cm) and vertically buried in the soil at each site. The height of the knee roots (the height from the ground to the apex of the knee roots) and average diameter at half the height of the knee roots were also measured. Because the surface of the knee roots was irregular, we carefully wrapped the knee roots exposed above the ground with tape (width, 1.62 cm). The surface area was calculated according to the length and width of the tape (with no overlap in the wrapping process). The survey of underground roots with

knee roots and without knee roots was randomly conducted in 15 plots (1 m × 1 m) within a range of 2 m from *T. ascendens*. The underground roots (depth, 0–50 cm) were excavated, cleaned, dried, and weighed.

Sampling of knee roots and assay of physiological indicators

In October 2016, the middle water table sites were chosen to investigate the development stages of the knee roots. The knee roots were divided into three stages on the basis of size and age: young-aged stage (Fig. 1A), middle-aged stage (Fig. 1B), and old-aged stage (Fig. 1C). The knee roots at the young-aged stage were less than 5 cm in height and less than 5 years of age. The knee roots at the middle-aged stage were 5 to 10 cm in height and 5 to 10 years of age. The knee roots at the old-aged stage were more than 10 cm in height and more than 10 years of age. The age of the knee roots was determined using the annual rings in the transverse section. The knee root samples were divided into two parts: the swollen part (upside) and non-swollen part (underside). Underground roots approximately 10 mm in diameter were collected as the control. The root tissues were randomly selected for physiological assay.

Ethylene release rate of the roots

Fresh root cambium tissues (0.6 g) were sealed in a closed bottle and incubated for 4 h at 30 °C. Then, gas samples (0.5 mL) were collected from the incubator to determine the ethylene concentration by using a gas chromatograph equipped with a flame ionization detector (FID) and electron capture

detector (ECD) (Agilent 7890A; Agilent Technologies Inc. USA). The external standard method was used to calculate the ethylene concentration of the samples.

ACC content

The ACC content was determined according to Hoffman et al. (1983). The root cambium tissue samples were cut into small pieces and mixed completely. Then, the samples (1.0 g) were homogenized in 8 mL of ethanol (95%) and centrifuged (8000 × *g*) at 4 °C for 15 min; the supernatant was transferred to a plastic bottle, 6 mL of ethanol (80%) was added to the residue and shaken for 30 min, the supernatant after centrifugation was transferred to the previous bottle, and the bottle was dried in a water bath at 40 °C. The dried residue was dissolved with 5 mL of distilled water and then centrifuged (8000 × *g*) at 4 °C for 10 min. The supernatant was used as the ACC fluid; 1 mL of the fluid and 40 μL of $HgCl_2$ (25 mmol·L^{-1}) were added into test tubes (20 mL) closed with rubber stoppers. Then, 1 mL of NaOCI-NaOH (v:v = 2:1) was injected into the test tubes with a syringe. The tubes were shaken for 10 min, and gas samples (0.5 mL) were collected from the tubes to determine the ethylene concentration via gas chromatography. The ACC concentration of fresh root samples was calculated using the following formula:

$$\text{ACC content (nmol·g}^{-1}\text{ FW)} = \frac{C \times V_L \times V}{R \times V_1 \times V_2 \times W \times 22.4}$$

where C is the ethylene concentration measured using gas chromatography (nL·L^{-1}); V_L is the volume of sample bottles without solution (mL); V is the volume of the extracting solution (mL); R is the transfer coefficient from ACC to ethylene; V_1 is the volume of the extracting solution used for

157 measurement (mL); V_2 is the gas sample volume for gas chromatography (mL); W is the fresh weight
158 of the root sample (g); and 22.4 is 1 molar gas constant under normal atmospheric conditions ($L \cdot mol^{-1}$).

159 **ACC synthase activity**

160 The ACC synthase activity was determined according to Mehta et al. (1988). Briefly, 1 g of root
161 cambium tissues were ground in a mortar with the extraction buffer (2 mL) and a small amount of
162 quartz sand at 4 °C and centrifuged at 10000 × *g*·for 20 min. The extraction buffer solution contained
163 400 $mmol \cdot L^{-1}$ potassium phosphate buffer solution (pH 8.5), 1 $mmol \cdot L^{-1}$ ethylene diamine tetraacetic
164 acid, 0.5% (v:v) β-mercaptoethanol, and 10 $\mu mol \cdot L^{-1}$ pyridoxal phosphate (PLP). The supernatant was
165 used to determine ACC enzyme activity; 0.4 mL of the enzyme extract and 1.6 mL of the buffer
166 solution (containing 50 $\mu mol \cdot L^{-1}$ SAM, 10 $\mu mol \cdot L^{-1}$ PLP, and 50 $mmol \cdot L^{-1}$ Hepes-KOH, pH 8.5) were
167 added to the test tubes and incubated at 32 °C for 1 h. Then, 0.1 mL of mercuric chloride (500
168 $mmol \cdot L^{-1}$) was added to stop the reaction, the test tubes were closed and incubated in ice water for 5
169 min, and 0.2 mL of 5% NaOCI-NaOH (v:v = 2:1) was injected into the test tubes with a syringe. The
170 test tubes were shaken for 10 min, and 0.5 mL gas sample was collected to determine the ethylene
171 content by using gas chromatography.

172 **ACC oxidase activity**

173 The ACC oxidase activity was determined according to Dong et al. (1992); 0.5 g of root cambium
174 tissues were ground in a mortar with the extraction buffer (2 mL) and a small amount of quartz sand at
175 4 °C and centrifuged at 12000 × *g*·for 10 min. The extraction buffer solution contained 100 $mmol \cdot L^{-1}$

Tris-HCl (pH 7.5), 10% (v:v) glycerin, 30 mmol·L^{-1} sodium ascorbate, 5% (v:v) polyvinylpyrrolidone, 0.1 mmol·L^{-1} $FeSO_4$, and 5 mmol·L^{-1} DTT. The supernatant was used to determine ACC oxidase activity; 0.2 mL of the enzyme extract and 1.8 mL of the buffer solution (containing 100 mmol·L^{-1} Tris-HCl (pH 7.5), 10% (v:v) glycerin, 30 mmol·L^{-1} sodium ascorbate, 30 mmol·L^{-1} $NaHCO_3$, 1.0 mmol·L^{-1} ACC, and 0.1 mmol·L^{-1} $FeSO_4$) were added to test tubes (20 mL) closed with rubber stoppers and incubated at 35 °C for 20 min. Then, 0.5 mL gas sample was collected to determine the ethylene content by using gas chromatography.

IAA content

The IAA content was determined according to Chen and Zhao (2008), and Yuan et al. (2008). First, 1 g of root cambium tissues were homogenized in liquid nitrogen and extracted in cold 80% methanol with butylated hydroxytoluene (1 mmol·L^{-1}) overnight at 4 °C, and centrifuged for 10000 × *g*·at the same temperature for 15 min. The supernatant was collected and passed through a C18 Sep-Pak Cartridge (Waters Corp., Milford, USA). The efflux was collected and dried in a rotary evaporator (RE-2000A, China). The residue was collected in 0.8 ml mobile phase (consisting of 23% (v:v) methanol and 23% (v:v) acetonitrile in double distilled water supplemented with 0.1% (v/v) phosphoric acid), filtered through a 0.25 mm filter and submitted for HPLC analysis. The IAA content was determined using the external standard method with a Waters 2695 Alliance HPLC (Waters Corp.). A Symmery C18 column (Waters Corp.) (4.6 × 250 mm, 5 μm) and a detection wavelength of

254 nm were used. A sample (50 μl) was automatically injected at a flow rate of 0.5 ml min^{-1}. Quantification was made by comparing the peak areas with the known amounts of IAA (Sigma).

Anatomical analysis of knee roots and underground roots

Three samples containing bark and currently produced xylem from the apex of knee roots at the middle-aged stage and mid-sized underground roots were obtained (Fig. 2). Small pieces (10 × 10 × 10 mm) of these root materials were fixed in FAA solution (formalin:acetic acid:ethanol:water, 5:5:60:30, v:v) for 24 h, rinsed in water, dehydrated in ethanol, and sealed in a paraffin block. The samples were transversely sectioned (10 μm) with a slide microtome (Leica RM2125RT, Germany), dewaxed, stained with safranin-fast green solution, and oven-dried at 40 °C. The anatomical structure of the samples was observed under a light microscope (Olympus, Japan), and the pictures were taken and processed using an image analysis software (DT2000, China).

Statistical analysis

The data were calculated and plotted using Microsoft Office Excel 2016, and all data were subjected to analysis of variance by using IBM SPSS Statistics 19.0. To determine the effects of the knee roots on the growth of *T. ascendens*, correlation analysis was performed using IBM SPSS Statistics 19.0. The data were presented as mean ± standard deviation (M ± SD) values, and differences in the data were evaluated using Duncan's test at a significance level of 0.05.

Results

Relationships between the morphological characteristics of knee roots and underground water table

The tree height, DBH, underground roots, and knee roots of *T. ascendens* were investigated, and the results showed that the formation and distribution of knee roots were significantly affected by the water table. The knee root density in the middle water table was 143.94% and 147.69% higher than that in the high water table and low water table, respectively. The height and diameter of the knee roots were also observed to be higher in the middle water table site (Table 1); thus, the middle water table significantly increased knee root formation and growth ($P < 0.05$).

Effects of the knee roots on the growth of *T. ascendens*

The weight of underground roots with knee roots was significantly higher than that of underground roots without knee roots (Fig. 3). Furthermore, the correlation between tree height and DBH and knee roots in the middle water table was analyzed; the height of *T. ascendens* was positively correlated with the number and size of knee roots (Table 2), and the DBH of *T. ascendens* was significantly positively correlated with the number and size of knee roots. The number of underground roots was positively correlated with the mean height and surface area of knee roots, and the weight of underground roots was significantly correlated with the mean height and surface area of knee roots.

Biochemical analysis of the roots

ACC content and ACC synthase and ACC oxidase enzyme activities

The ACC content in the knee roots at different development stages did not show significant differences ($P > 0.05$): KY > KM > KO (Fig. 4A). However, the ACC content was significantly lower in the knee roots than in the underground roots ($P < 0.05$). The ACC synthase activity showed the same trend as ACC content and was not significantly different among the development stages of the knee roots (Fig. 4B), and the ACC synthase activity was significantly lower in the knee roots than in the underground roots ($P < 0.05$). The ACC oxidase activity in the knee roots at different development stages was in the order of KY > KM > KO, and ACC oxidase reduced with the growth of knee roots (Fig. 4C). The ACC oxidase activity was significantly higher in the knee roots than in the underground roots, except in KO (Fig. 4C; $P < 0.05$).

Endogenous hormone release rates

Different ethylene release rates were observed in the underground roots and knee roots (Fig. 5A). The ethylene release rate at different stages was significantly higher in the knee roots than in the underground roots ($P < 0.05$). In addition, significant differences were observed among the different development stages of the knee roots ($P < 0.05$). The maximum ethylene release rate from the knee roots was observed in KO, and the minimum, in KM.

The IAA content was in the order of UR > KM > KO > KY (Fig. 5B), with no statistically significant differences between UR and KM ($P > 0.05$) and KO and KY ($P > 0.05$).

Anatomical structure of the knee roots and underground roots

248 The knee roots had 3-4 layers of rhytidome, which were formed by the integration of the
249 periderm and phloem, and some parts of the periderm had branches (Fig. 6). The periderm was
250 composed of many layers of cork cells, and the cork layer, cork-forming layer, and inner cork layer
251 were closely overlapped. The phloem, isolated from the periderm on the apex side of the knee roots,
252 was dead, the cells were broken, and the arrangement of cells was loose and porous. The phloem
253 parenchyma cells were close to the cambium and rectangular. The cell wall of the phloem fiber was
254 thickened and showed an increase in lignification. The phloem ray expanded obviously, and the
255 arrangement was loose. The knee roots were mainly composed of the secondary xylem; in the cross-
256 section, xylem tracheids were arranged in order; the early tracheids were rectangular, square, or
257 polygonal; the late tracheids were obviously smaller than the early tracheids; and the cell wall was
258 thicker. The rhytidome layers of the underground roots were lesser than those of the knee roots (1-2
259 layers). The width of the phloem was smaller than that of the knee roots; the xylem tracheids were
260 arranged in order, and the shape was similar to that of the knee roots.

261 **Discussion**

262 In plants, flood tolerance is related to shifts in anatomical and morphological characteristics
263 (Blom and Voesenek 1996, Hua et al. 2017). Under flooding conditions, the formation of knee roots is
264 a morphological adaptation of *T. ascendens* to environmental stress (Fig. 7). *Taxodium ascendens* with
265 knee roots had more underground roots and showed better tree growth, which suggests that the knee
266 roots are beneficial for the growth of *T. ascendens*. Our results suggest that the middle water table is

267 more suitable for the formation and growth of knee roots, which is consistent with the findings of
268 Tang et al. (2008) who reported that *T. ascendens* formed aerating roots in the high water table and
269 knee roots in the middle water table.

270 Ethylene production plays an important role in modifying the plant response to flooding stress
271 (Zhou et al. 2020). Ethylene induces the genes of enzymes associated with aerenchyma formation
272 (Drew et al. 1979, Brailsford et al. 1993, Sairam et al. 2008). Ethylene synthesis includes two
273 important processes: catalysis of *S*-adenosylmethionine (SAM) to ACC by ACC synthase and catalysis
274 of ACC to ethylene by ACC oxidase. ACC synthesis does not require oxygen; in fact, ACC synthase
275 activity is stimulated in roots under flood conditions (Cohen and Kende 1987, Dong et al. 1992, Zhou
276 et al. 2001; Williams and Golden 2002). In our study, the underground roots of *T. ascendens* were
277 exposed to anoxic conditions for a long time; expression of the ACC synthetase gene was stimulated
278 by anaerobic stress (Van der Straeten et al. 2001, Rieu et al. 2005), which increased ACC synthetase
279 activity in the underground roots. However, the knee roots were exposed to air in October (sampling
280 time); thus, the activity of ACC synthetase was significantly lower in the knee roots than in the
281 underground roots. The conversion of ACC to ethylene has an obligate requirement for oxygen, and
282 ACC oxidase can also be induced by anoxic stress (Vriezen et al. 1999, Bailey-Serres and Voesenek
283 2008, Buttò et al. 2020). Thus, our results suggest that the oxygen status was improved by the
284 formation and development of knee roots, ACC oxidase activity decreased with the development of
285 knee roots, knee roots at the young-aged stage showed the highest ACC oxidase activity, knee roots at

286 the old-aged stage may be less affected by flooding stress, and showed the lowest ACC oxidase
287 activity. When the underground roots of *T. ascendens* were exposed to flooding in the growing season,
288 the activity of ACC synthase was enhanced by anaerobic stress, which led to the accumulation of ACC.
289 When the water table receded, the upper surface of the roots distributed in the shallow soil received
290 oxygen, and the ACC was transported to better-aerated tissues. This resulted in ethylene synthesis by
291 ACC oxidase; ethylene promoted the uneven growth of morphologically upper and lower roots,
292 leading to the formation of knee roots. Thus, the knee roots had significantly higher ethylene content
293 than the underground roots (Fig. 5A), and the highest ethylene content was observed in the old-aged
294 stage of the knee roots. This is consistent with the results of Pesquet and Tuominen (2011), who
295 reported that the ethylene content was maximum before cell death and lignification. The knee roots
296 formed easily when the tree was exposed to anoxic conditions (reduction state) and aerobic conditions
297 (oxidation state) alternately. Thus, our results suggest that the high water table (the underground roots
298 experienced flooding from June to September, and the soil was in the reduction state during the
299 growing season) and low water table (no flooding throughout the year, and the soil was in oxidation
300 state) are not suitable for the formation of knee roots; only the middle water table (flooding period was
301 1 to 2 months from July to August, and the annual average water table was from -0.6 m to -1.2 m) is
302 suitable for the formation of knee roots. Moreover, ACC and some related enzymes were found in the
303 knee root tissues, suggesting that the formation and development of *T. ascendens* knee roots are
304 related to ethylene production and accumulation.

305 The phytohormone IAA is essential for root development and adventitious root formation (Visser
306 and Voesenek 2004, Kitomiy et al. 2008). IAA also plays an important role in the development and
307 activities of the cambium (Uggla et al. 1998, Bhalerao and Fischer 2014). Our study suggests that,
308 with the development of the knee roots, the IAA content first increased and then decreased; IAA
309 content was lower in the knee roots at the young-aged and old-aged stages and higher in those at the
310 middle-aged stage. High IAA content is beneficial for cambium cell enlargement, expansion, and
311 division (Bhalerao and Fischer 2016), whereas low IAA content is beneficial for secondary cell-wall
312 deposition and lignification (Fajstavr et al. 2018). Our results were similar to the conclusion of Cui et
313 al. (1999, 2000), who reported that endogenous IAA concentration in the cambium of *Broussonetia*
314 *papyrifera* increased obviously when the cambium formed the immature phloem and xylem and
315 decreased when the immature vascular cells differentiated towards maturation; this indicates IAA
316 concentrations are different in the division stage of cambium cells and differentiation stage of
317 cambium derivative cells.

318 Under flood conditions, anoxia stimulates the production of ethylene, which accumulates in roots
319 surrounded by water and induces programmed cell death in the cortex tissue (He et al. 1996, Drew et
320 al. 2000). In our study, the cells of the periderm at the apex of the knee roots were dead, arranged
321 loosely, and had a large number of intercellular spaces, which is conducive to gas exchange between
322 the knee roots and air. Because the knee roots were exposed to air to resist the adverse effects of
323 external environmental factors, the periderm of the knee roots was obviously thicker than that of the

underground roots. Plant stems can form irregular wide rays composed of abnormally large ray cells after the application of ethephon (Pallardy 2011). Because the knee roots were stimulated by ethylene, phloem rays at the apex of the knee roots expanded obviously when compared with the underground roots. Thus, the flooding resistance of *T. ascendens* is related to the formation of knee roots and enhancement of air permeability. Although this study showed that ACC, ethylene, and IAA affected the formation of knee roots, the underlying molecular mechanism is still unclear. We recommend the transcription factors and gene expression of *T. ascendens* roots should be explored to further understand the mechanism of flooding resistance.

Conclusions

Our results suggest that the formation and distribution of knee roots are significantly affected by the water table. The middle water table significantly enhanced the formation and distribution of knee roots in *T. ascendens*. Furthermore, the knee roots were beneficial for the growth of *T. ascendens*, and the height and the DBH of *T. ascendens* were positively correlated with the number and size of knee roots. The ACC content and ACC synthase activities in the knee roots at different development stages did not show any significant differences, whereas they were significantly lower in the knee roots than in the underground roots. The ACC oxidase activities in the knee roots decreased as the knee roots developed. Ethylene and IAA affected the formation of knee roots. The ethylene release rate was significantly higher in the knee roots than in the underground roots, and the IAA content first increased and then decreased with the development of the knee roots. The anatomical structure of the

knee roots showed that cells of the periderm at the apex of the knee roots were dead, arranged loosely, and had a large number of intercellular spaces that improved internal gas diffusion. In conclusion, seasonal flooding induced the production of endogenous hormones, resulting in the formation of knee root, which improved root respiration and ventilation, thus improving the flooding tolerance of *T. ascendens*.

Conflicts of Interest

The authors declare no conflict of interest.

Acknowledgement

This study was funded by the National Natural Science Foundation of China (No. 31170566) and the Priority Academic Program Development of Jiangsu Higher Education Institutions (PAPD).

References

Andrson PH, Pezeshki SR (1999) The effects of intermittent flooding on seedlings of three forest species. Photosynthetica 37(4): 543-552.

Bailey-Serres J, Voesenek LACJ (2008) Flooding stress: Acclimations and genetic diversity. Annu Rev Plant Biol 59: 313-339.

Bhalerao RP, Fischer U (2014) Auxin gradients across wood—instructive or incidental? Physiol Plant 151: 43-51

Bhalerao RP, Fischer U (2016) Environmental and hormonal control of cambial stem cell dynamics. J Exp Bot 68(1): 79-87.

362 Blom CW, Voesenek LA (1996) Flooding: the survival strategies of plants. Trends Ecol Evol 11(7):
363 290-295.
364 Bouma TJ, Nielsen KL, Van Hal J, Koutstaal B (2001) Root system topology and diameter
365 distribution of species from habitats differing in inundation frequency. Funct Ecol 15(3): 360-369.
366 Brailsford, RW, Voesenek LACJ, Blom CWPM, Smith AR, Hall MA, Jackson MB (1993) Enhanced
367 ethylene production by primary roots of *Zea mays* L. in response to sub-ambient partial pressure
368 of oxygen. Plant Cell Environ 16: 1071-1080.
369 Buttò V, Deslauriers A, Rossi S, Rozenberg P, Shishov V, Morin H (2020) The role of plant hormones
370 in tree-ring formation. Trees 34(2) doi:10.1007/s00468-019-01940-4
371 Chen D, Zhao J (2008) Free IAA in stigmas and styles during pollen germination and pollen tube
372 growth of *Nicotiana tabacum*. Physiol Plantarum 134(1): 202–215.
373 Cohen E, Kende H (1987) In vivo 1-aminocyclopropane-1- carboxylate synthase activity in internodes
374 of deep water rice: Enhancement by submergence and low oxygen levels. Plant Physiol 84: 282-
375 286.
376 Conner WH, McLeod KW, McCarron JK (1997) Flooding and salinity effects on growth and survival
377 of four common forested wetland species. Wetl Ecol Manag 5(2): 99-109.
378 Cui K, Wang X, Duan J, Wang SY (1999) Change of endogenous IAA during cambial activity and
379 IAA binding protein in cambial cells in *Broussonetia papyrifera*. Acta Botanica Sinica 41(10):
380 1082-1085. (in Chinese)

381 Cui K, Wang X, Duan J (2000) Change in the concentration and tissue - localization of endogenous
382 IAA during the regeneration after girdling in *Broussonetia papyrifera* (L.) Vent. Acta
383 Scientiarum Naturalium Universitatis Pekinensis 36(4): 495-502. (in Chinese)
384 Dong JG, Fernández-Maculet JC, Yang SF (1992) Purification and characterization of 1-
385 aminocyclopropane-1-carboxylate oxidase from apple fruit. P Natl Acad Sci USA 89(20): 9789-
386 9793.
387 Drew MC, He CJ, Morgan PW (2000) Programmed cell death and aerenchyma formation in roots.
388 Trends Plant Sci 5: 123-127.
389 Drew MC, Jackson MB, Giffard S (1979) Ethylene-promoted adventitious rooting and development of
390 cortical air spaces (aerenchyma) in roots may adaptive responses to flooding in *Zea mays* L.
391 Planta 147: 83-88.
392 Du Q, Zhong QC, Wang KY (2010) Root effect of three vegetation types on shoreline stabilization
393 of Chongming Island, Shanghai. Pedosphere 20(6): 692–701.
394 Fajstavr M, Paschová Z, Giagli K, Vavrčík H, Gryc V, Urban J (2018) Auxin (IAA) and soluble
395 carbohydrate seasonal dynamics monitored during xylogenesis and phloemogenesis in Scots pine.
396 iForest 11: 553-562.
397 He CJ, Finlayson SA, Drew MC, Jordan WR, Morgan PW (1996) Ethylene biosynthesis during
398 aerenchyma formation in roots of maize subjected to mechanical impedance and hypoxia. Plant
399 Physiol 112: 1679-1685.

400 Herzog M, Striker GG, Colmer TD, Pedersen O (2016) Mechanisms of waterlogging tolerance in
401 wheat - a review of root and shoot physiology. Plant Cell Environ 39(5): 1068-1086.
402 Hirabayashi Y, Mahendran R, Koirala S, Konoshima L, Yamazaki D, Watanabe S, Kanae S (2013)
403 Global flood risk under climate change. Nat Clim Change 3(9): 816-821.
404 Hoffman NE, Liu Y, Yang SF (1983) Changes in 1- (malonylamino) cyclopropane-1-carboxylic acid
405 content in wilted wheat leaves in relation to their ethylene production rates and 1-
406 aminocyclopropane-1-carboxylic acid content. Planta 157(6): 518-523.
407 Hua J, Han L, Wang Z, Gu C, Yin Y (2017) Morpho-anatomical and photosynthetic responses of
408 *Taxodium* hybrid 'Zhongshanshan' 406 to prolonged flooding. Flora 231: 29-37.
409 Jackson MB (2007) Ethylene-promoted elongation: an adaptation to submergence stress. Ann Bot-
410 London 101: 229-248.
411 Khan M, Iqbal R, Trivellini A, Chhillar H, Chopra P, Ferrante A, Khan NA, Ismail AM (2020) The
412 significance and functions of ethylene in flooding stress tolerance in plants. Environ Exp Bot
413 104188. doi:10.1016/j.envexpbot.2020.104188
414 Kitomiy Y, Ogawa A, Kitanoh I, Inukai Y (2008) *CRL4* regulates crown root formation through auxin
415 transport in rice. Plant Root 2: 19-28.
416 Kuai J, Zhou Z, WangY, Meng Y, Chen B, Zhao W (2015) The effects of short-term waterlogging on
417 the lint yield and yield components of cotton with respect to boll position. Europ J Agronomy 67:
418 61-74.

419 Lance SE, Alison B (2010) Characterization of cork warts and aerenchyma in leaves of *Rhizophova*
420 *mangle* and *Rhizophora racemosa*. J Torrey Bot Soc 137(1): 30-38. doi:10.2307/40864968
421 Li C, Zhong Z, Geng Y, Schneider R (2010) Comparative studies on physiological and biochemical
422 adaptation of *Taxodium distichum* and *Taxodium ascendens* seedlings to different soil water
423 regimes. Plant Soil 329: 481-494.
424 Liu D, Liu S, Yi P, Yin H, Xie B, Liu Z (2019) Effects of exogenous hormones on physiological
425 characteristics of root system of Muskmelon seedlings under flooding stress. Jiangsu Agricultural
426 Sciences 47(9): 182-185. (in Chinese)
427 Mehta AM, Jordan RL, Anderson JD, Mattoo AK (1988) Identification of a unique isoform of 1-
428 aminocyclopropane -1-carboxylic acid synthase by monoclonal antibody. P Natl Acad Sci USA
429 85(23): 8810-8814.
430 Mendez-Alonzo R, Moctezuma C, Ordonez VR, Angeles G, Martinez AJ, Lopez-Portillo J (2015)
431 Root biomechanics in Rhizophora mangle: anatomy, morphology and ecology of mangrove's
432 flying buttresses. Ann Bot-London 115(5): 833-840.
433 Pallardy SG (2011) Physiology of woody plants. Science Press, Beijing.
434 Pesquet E, Tuominen H (2011) Ethylene stimulates tracheary element differentiation in *Zinnia elegans*
435 cell cultures. New Phytol 190: 138-149.
436 Purnobasuki H, Suzuki M (2005) Aerenchyma tissue development and gas-pathway structure in root
437 of *Avicennia marina* (Forsk.) Vierh. J Plant Res 118(4): 285-294.

438 Purnobasuki H, Purnama PR, Kobayashi K (2017) Morphology of four root types and anatomy of
439 root-root junction in relation gas pathway of *Avicennia marina* (Forsk) Vierh roots. International
440 Journal of Plant Research 30(2): 100. doi: 10.5958/2229-4473.2017.00143.4
441 Rieu I, Cristescu SM, Harren FJM, Huibers W, Voesenek LACJ, Mariani C, Vriezen WH (2005) RP-
442 ACS1, a flooding-induced 1-aminocyclopropane-1-carboxylate synthase gene of *Rumex palustris*,
443 is involved in rhythmic ethylene production. J Exp Bot 56: 841-849.
444 Sairam RK, Kumutha D, Ezhilmathi K, Deshmukh PS, Srivastava GC (2008) Physiology and
445 biochemistry of waterlogging tolerance in plants. Bio Plantarum 52(3): 401-412.
446 Sakio H, Yamamoto F (2002) Ecology of riparian forests. University of Tokyo Press, Tokyo.
447 Sena Gomes AR, Kozlowski TT (1980) Effects of flooding on *Eucalyptus camaldulensis* and
448 *Eucalyptus globulus* seedlings. Oecologia 46(2): 139-142.
449 Sundberg B, Little CH, Cui K, Sandberg G (1991) Level of endogenous indole-3-acetic acid in the
450 stem of *Pinus sylvestris* in relation to the seasonal variation of cambial activity. Plant Cell
451 Environ 14(2): 241-246.
452 Tang LZ, Huang BL, Haibara K, Toda H (2008) Ecological adaption mechanisms of roots to flooded
453 soil and respiration characteristics of knee roots of *Taxodium ascendens.* Journal of Plant Ecology
454 32(6): 1258-1267. (in Chinese)
455 Uggla C, Mellerowicz EJ, Sundberg B (1998) Indole-3-acetic acid controls cambial growth in Scots
456 pine by positional signaling. Plant Physiol 117(1): 113-121.

457 Vall-llaura N, Giné-Bordonaba J, Usall J, Larrigaudière C, Teixidó N, Torres R (2020) Ethylene
458 biosynthesis and response factors are differentially modulated during the interaction of peach
459 petals with *Monilinia laxa* or *Monilinia fructicola*. Plant Sci 299: 110599.
460 doi:10.1016/j.plantsci.2020.110599
461 Van der Straeten D, Zhou Z, Prinsen E, Van Onckelen HA, Van Montagu MC (2001) A comparative
462 molecular physiological study of submergence response in lowland and deepwater rice. Plant
463 Physiol 125: 955-968.
464 Visser EJW, Voesenek LACJ (2004) Acclimation to soil flooding – sensing and signal-transduction.
465 Plant Soil 254: 197-214.
466 Voesenek LA, Baileyserres J (2013) Flooding tolerance: O_2 sensing and survival strategies. Curr Opin
467 Plant Biol 16: 647-653.
468 Vriezen WH, Hulzink R, Mariani C, Voesenek LACJ (1999) 1-Aminocyclopropane-1-carboxylate
469 oxidase activity limits ethylene biosynthesis in *Rumex palustris* during submergence. Plant
470 Physiol 121: 189-195.
471 Wang C, Li C, Hong W, Wei X, Han W (2016) Effects of long-term periodic submergence on
472 photosynthesis and growth of *Taxodium distichum* and *Taxodium ascendens* saplings in the
473 hydro-fluctuation zone of the Three Gorges Reservoir of China. Plos One 11(9): e0162867.
474 Williams OJ, Golden KD (2002) Purification and characterization of ACC oxidase from *Artocarpus*
475 *altilis*. Plant Physiol Bioch 40(4): 273-279.

476 Xiong Q, Cao C, Shen T, Zhong L, He H, Chen X (2019) Comprehensive metabolomic and proteomic
477 analysis in biochemical metabolic pathways of rice spikes under drought and submergence stress.
478 BBA - Proteins Proteom 1867: 237-247.
479 Yamamoto F (1992) Effects of depth of flooding on growth and anatomy of stems and knee roots of
480 *Taxodium distichum*. IAWA J 13(1): 93-104. doi: 10.1163/22941932-90000560
481 Yi YH, Fan DY, Xie ZQ, Chen FQ (2008) The effects of waterlogging on photosynthesis-related eco-
482 physiological processes in the seedlings of *Quercus variabilis* and *Taxodium ascendens*. Acta
483 Ecologica Sinica 28(12): 6025-6033.
484 Yuan J, Chen D, Ren YJ, Zhang XL, Zhao J (2008) Characteristic and expression analysis of a
485 metallothionein gene, OsMT2b, down-regulated by cytokinin suggest functions in root
486 development and seed embryo germination of rice (*Oryza sativa* L.). Plant Physiol 146: 1637–
487 1650
488 Zhou Z, Vriezen W, Van Caeneghem W, Montagu MV, Straeten DVD (2001) Rapid induction of a
489 novel ACC synthase gene in deepwater rice seedlings upon complete submergence. Euphytica
490 121(2): 137-143.
491 Zhou W, Chen F, Meng Y, Chandrasekaran U, Luo X, Yang W, Shu K (2020) Plant
492 waterlogging/flooding stress responses: From seed germination to maturation. Plant Physiol
493 Bioch 148: 228-236.
494

Table 1 Number and size of knee roots of *Taxodium ascendens* at different water table sites

Site	Annual Water Table (m)	Flooding Period (month year^{-1})	Knee Root Density (root m^{-2})	Knee Root Height (cm)	Knee Root Diameter (cm)
High water table	> -0.6	>3	0.66±0.02 b	6.65±1.36 b	3.73±0.12 b
Middle water table	-0.6 to -1.2	1 to 2	1.61±0.64 a	7.64±1.42 a	4.11±0.51 a
Low water table	< -1.2	0	0.65±0.02 b	6.72±1.60 b	3.70±0.25 b

Data represent mean ± standard deviation values of seven replication sites.

Values followed by the same letter are not significantly different at $P < 0.05$, according to Duncan's multiple range tests. The height of the knee roots refers to the height from the ground to the apex of the knee roots. The knee root diameter refers to the average diameter at half the height of the knee roots.

Table 2 Correlation coefficient between number and size of knee roots and DBH and tree height of *Taxodium ascendens* at Zhaoguan Forest Farm

	Number of knee roots	Mean height of knee roots	Mean diameter of knee roots	Surface area of knee roots
Tree height	0.45*	0.46*	0.52*	0.52*
Tree DBH	0.66**	0.61**	0.65**	0.59**
Number of underground roots		0.87*	0.48	0.86*
Weight of underground roots		0.93**	0.53	0.95**

DBH, diameter at breast height. *P = 0.05 significance; **P = 0.01 significance.

509

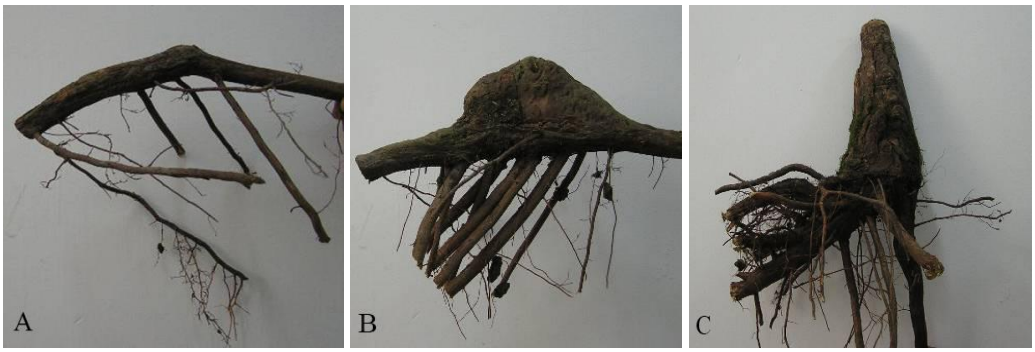

510

511 Fig. 1 Photographs of knee roots of young-aged stage (A), middle-aged stage (B), and old-aged stage
512 (C).

Fig. 2 Photographs of a root segment with a knee root (left) and transverse section of a knee root (right).

Vertical bars indicate the portion with the transverse section of the knee root. Letters indicate positions of samples for microscopic observations. A, apex.

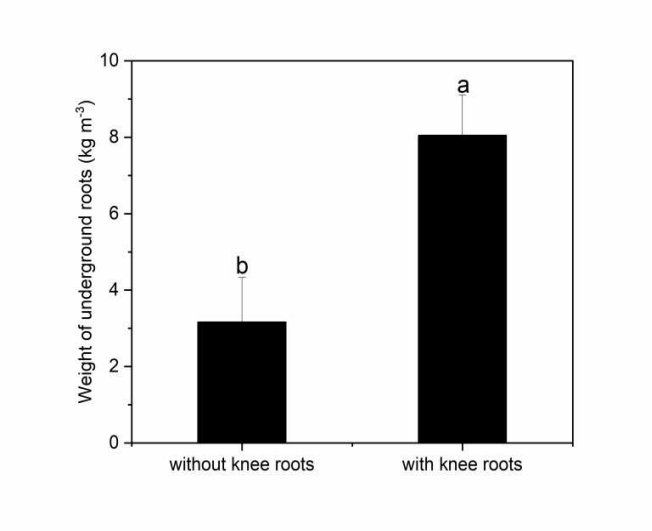

Fig. 3 Weight of underground roots with or without knee roots

Values followed by the same letter(s) are not significantly different at $P < 0.05$, according to Duncan's multiple range tests. Error bars are standard error of the mean; n = 3.

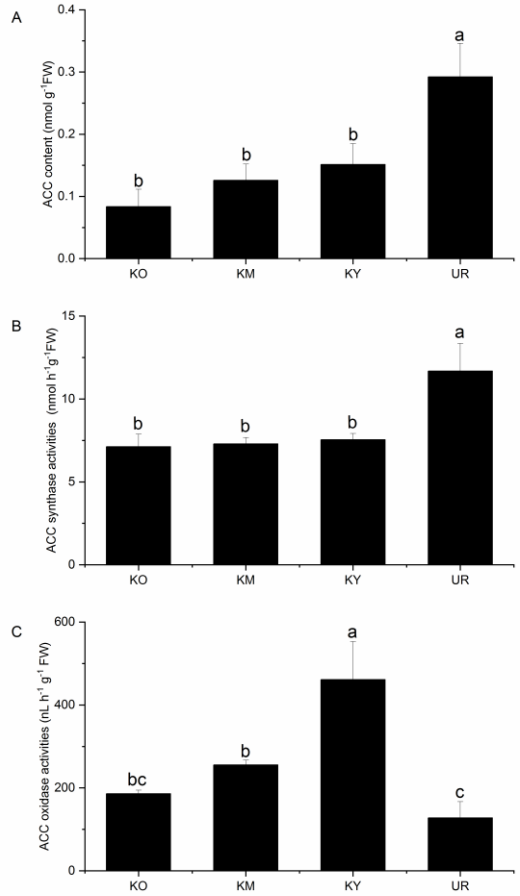

Fig. 4 ACC content and ACC synthase and ACC oxidase activities in different roots of *Taxodium ascendens* (KO, KM, and KY refer to the knee roots at different development stages: old-aged stage, middle-aged stage, and young-aged stage, respectively. UR means underground roots.). Values followed by the same letter(s) are not significantly different at $P < 0.05$, according to Duncan's multiple range tests. Error bars are standard error of the mean; n = 3.

536

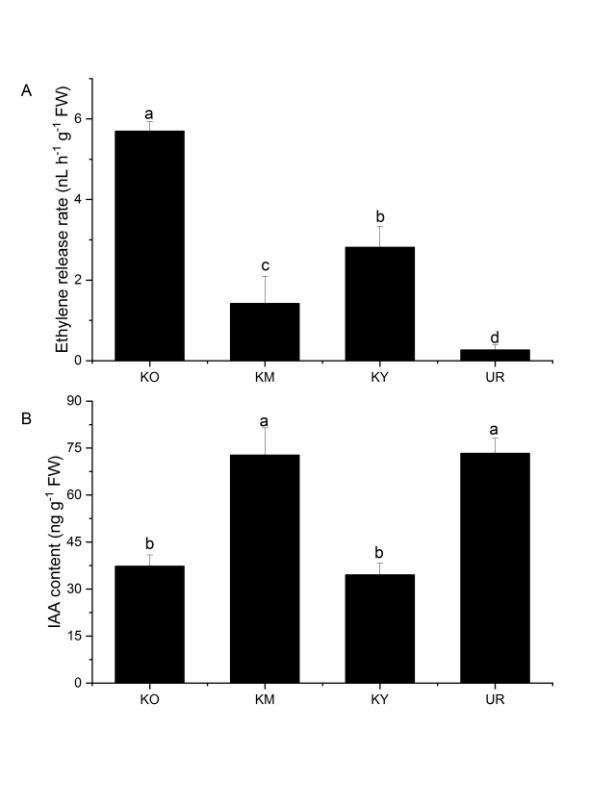

537

538 **Fig. 5** Ethylene release rates from different root types of *Taxodium ascendens*

539

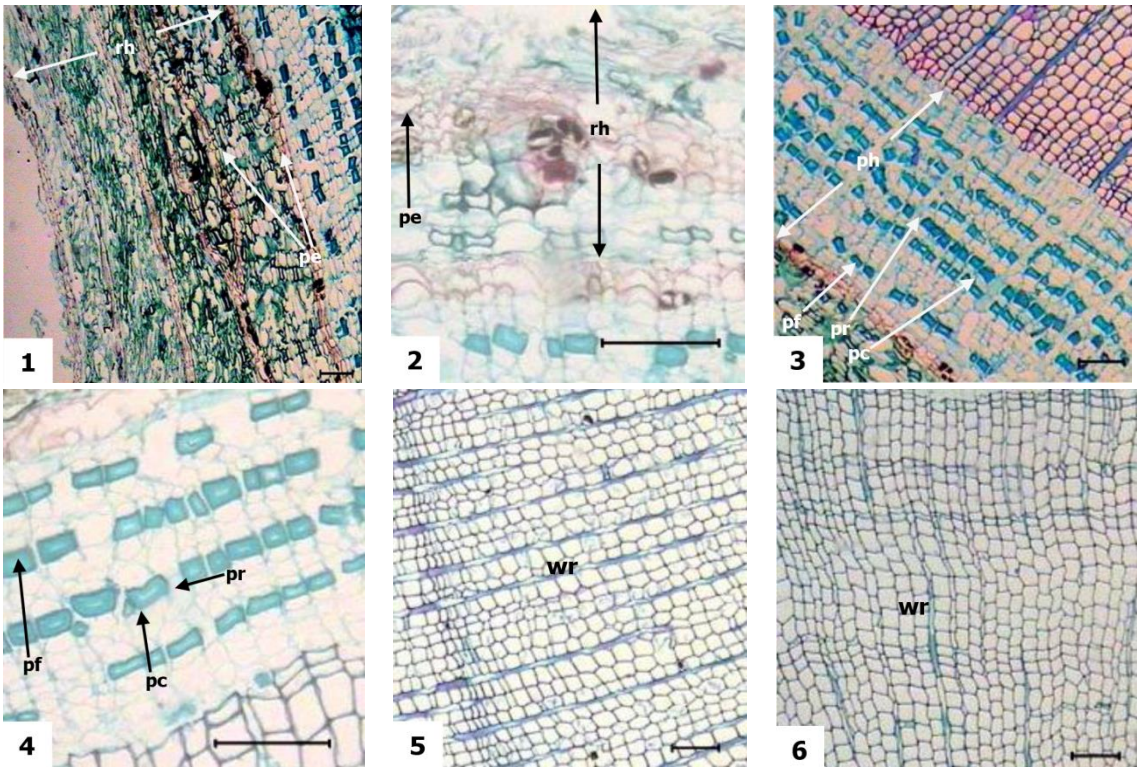

Fig. 6 Transverse anatomical structure of knee roots and underground roots

Horizontal line = 100 μm. 1, Rhytidome at the apex of the knee roots (middle stage); 2, rhytidome of mid-sized underground roots; 3, phloem at the apex of the knee roots (middle stage); 4, phloem of mid-sized underground roots; 5, xylem at the apex of the knee roots (middle stage); 6, xylem of mid-sized underground roots; rh: rhytidome; pe: periderm; ph: phloem; pr: phloem ray; pf: phloem fiber; pc: phloem parenchyma cell; wr: wood ray.

550

551

552 **Fig. 7** Knee roots of *Taxodium ascendens* in the wetland

553

Figures

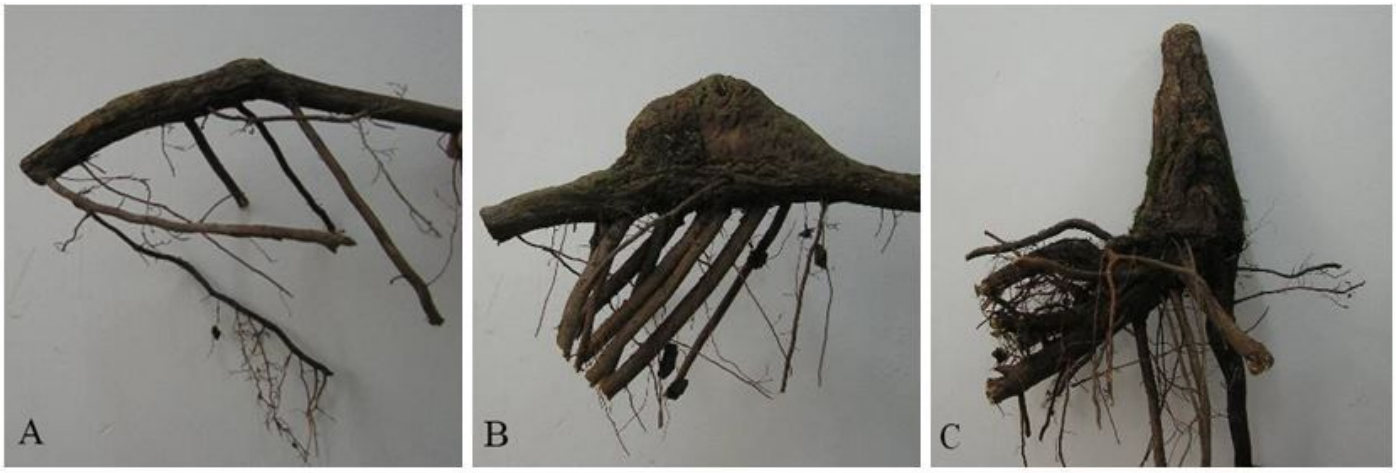

Figure 1

Photographs of knee roots of young-aged stage (A), middle-aged stage (B), and old-aged stage (C).

Figure 2

Photographs of a root segment with a knee root (left) and transverse section of a knee root (right). Vertical bars indicate the portion with the transverse section of the knee root. Letters indicate positions of samples for microscopic observations. A, apex.

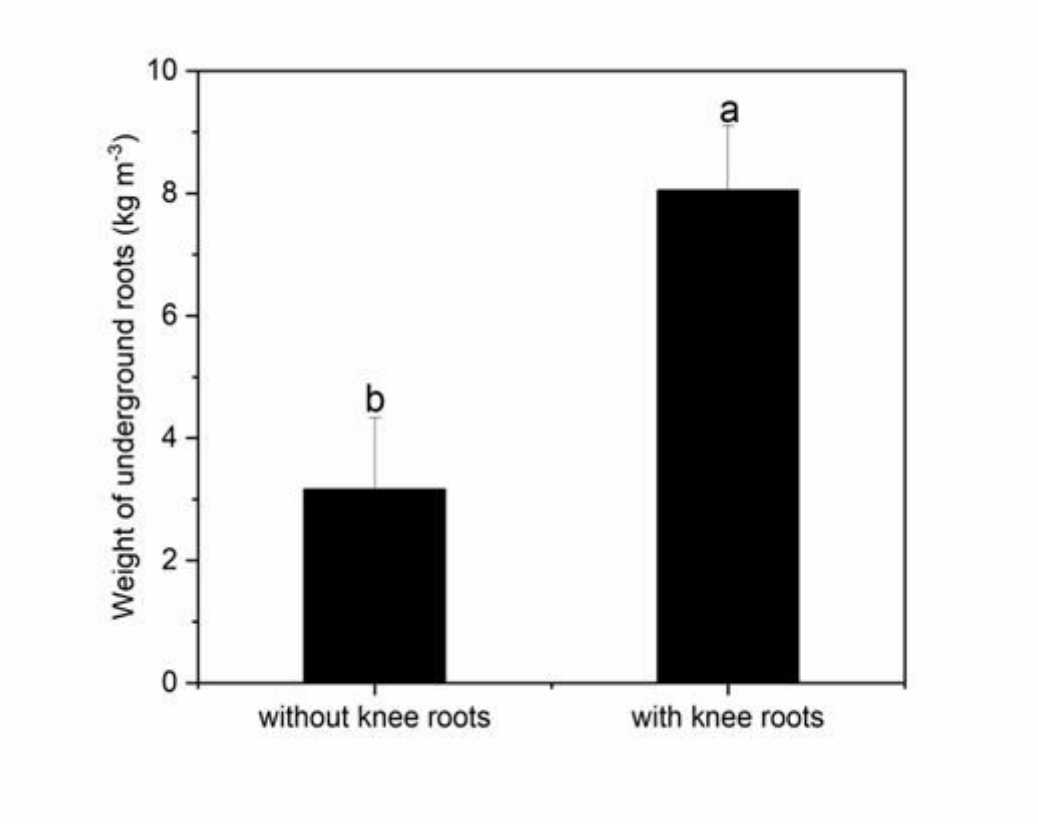

Figure 3

Weight of underground roots with or without knee roots Values followed by the same letter(s) are not significantly different at $P < 0.05$, according to Duncan's multiple range tests. Error bars are standard error of the mean; $n = 3$.

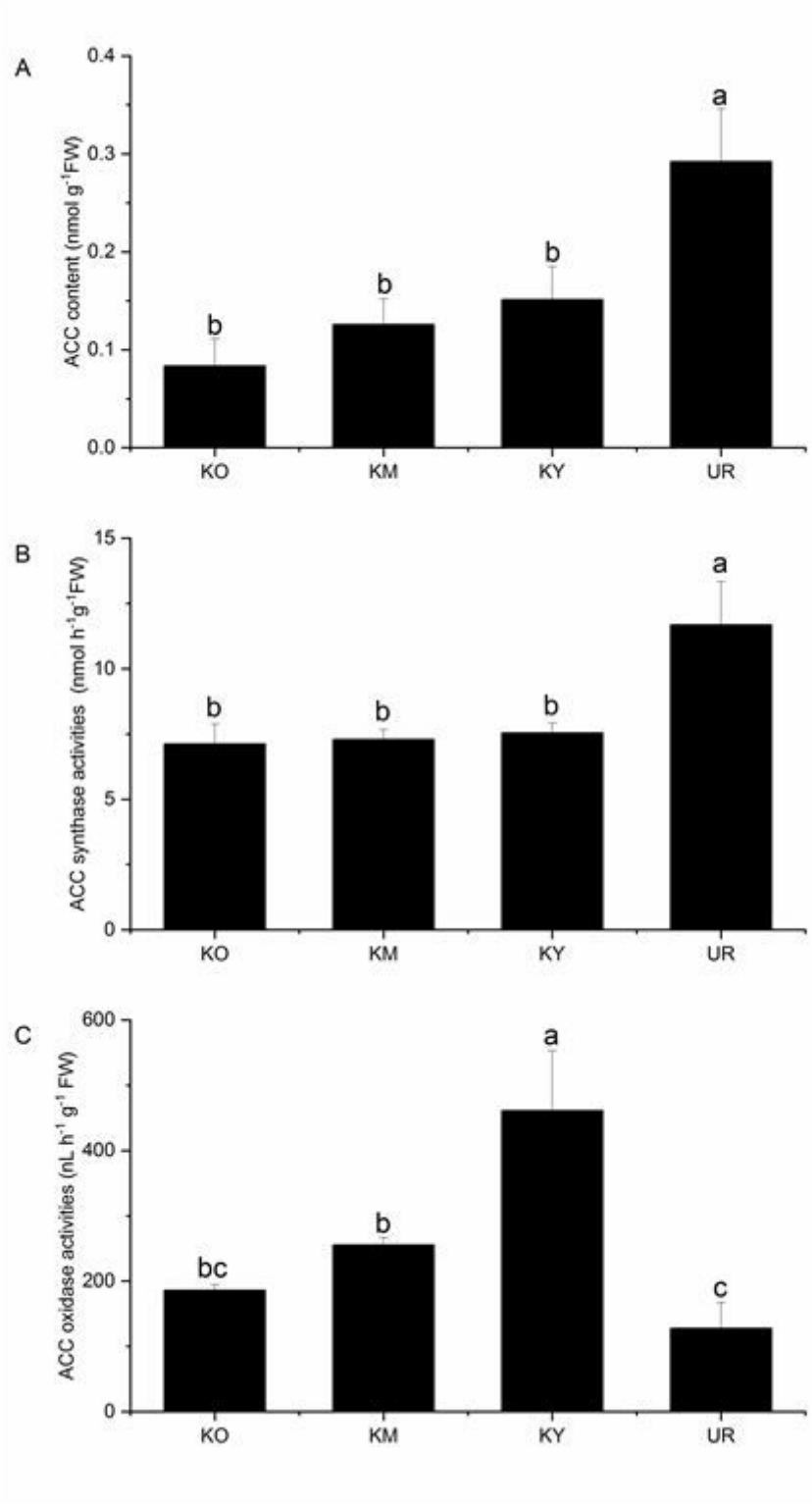

Figure 4

ACC content and ACC synthase and ACC oxidase activities in different roots of Taxodium ascendens (KO, KM, and KY refer to the knee roots at different development stages: old-aged stage, middle-aged stage, and young-aged stage, respectively. UR means underground roots.). Values followed by the same letter(s) are not significantly different at $P < 0.05$, according to Duncan's multiple range tests. Error bars are standard error of the mean; n = 3.

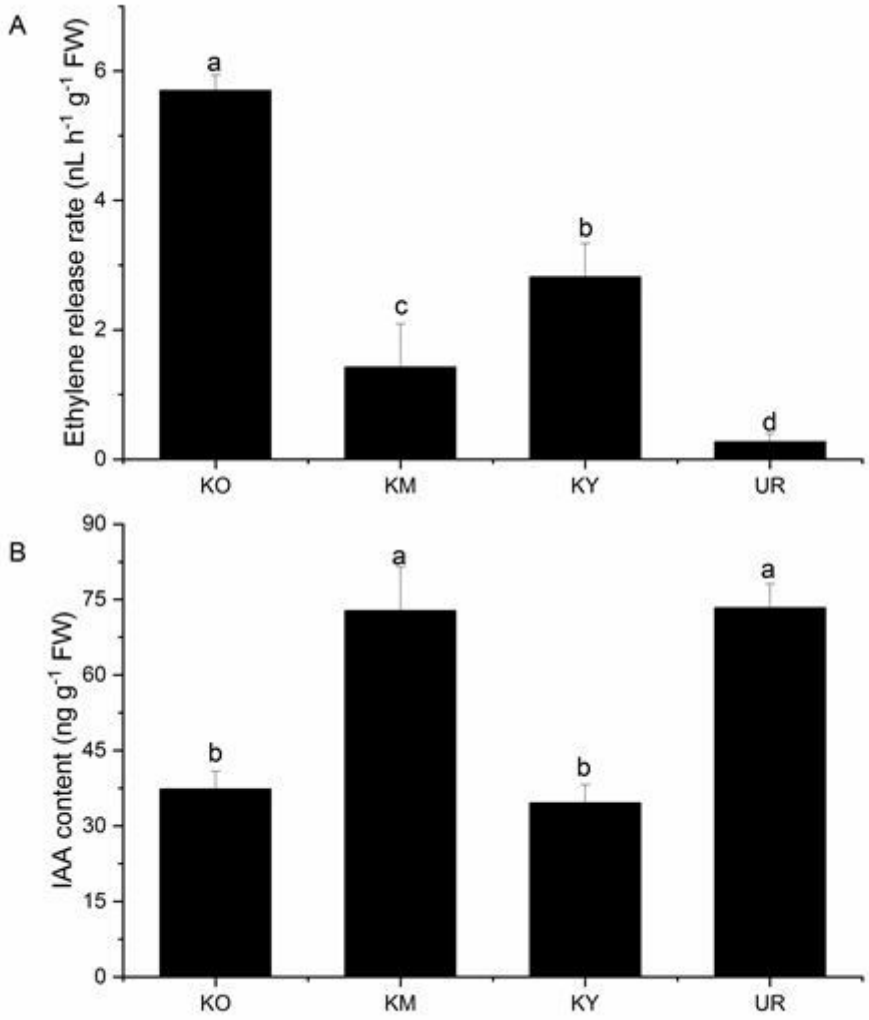

Figure 5

Ethylene release rates from different root types of Taxodium ascendens

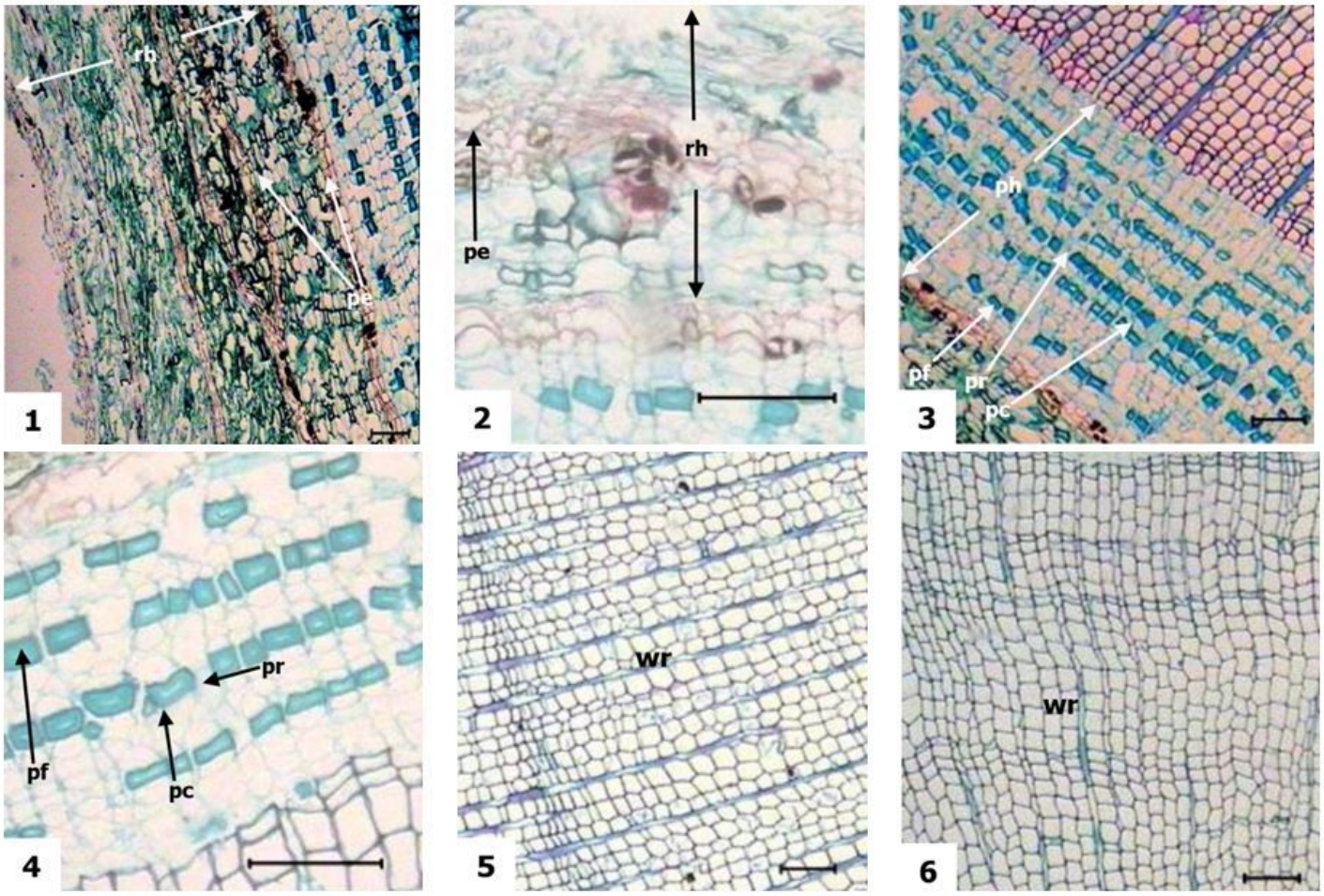

Figure 6

Transverse anatomical structure of knee roots and underground roots Horizontal line = 100 μm. 1, Rhytidome at the apex of the knee roots (middle stage); 2, rhytidome of mid-sized underground roots; 3, phloem at the apex of the knee roots (middle stage); 4, phloem of mid-sized underground roots; 5, xylem at the apex of the knee roots (middle stage); 6, xylem of mid-sized underground roots; rh: rhytidome; pe: periderm; ph: phloem; pr: phloem ray; pf: phloem fiber; pc: phloem parenchyma cell; wr: wood ray.

Figure 7

Knee roots of Taxodium ascendens in the wetland